Published in final edited form as:
Nat Immunol. 2014 December ; 15(12): 1116–1125. doi:10.1038/ni.3023.

Chitinase-like proteins promote IL-17-mediated neutrophilia in a trade-off between nematode killing and host damage

Tara E. Sutherland[1], **Nicola Logan**[1], **Dominik Rückerl**[1], **Alison A. Humbles**[2], **Stuart M. Allan**[3], **Venizelos Papayannopoulos**[4], **Brigitta Stockinger**[4], **Rick M. Maizels**[1], and **Judith E. Allen**[1]

[1]Institute of Immunology and Infection Research, Centre for Immunity Infection and Evolution, School of Biological Sciences, University of Edinburgh, Edinburgh, EH9 3FL, UK

[2]Department of Respiratory, Inflammation & Autoimmunity, MedImmune LLC, Gaithersburg, Maryland, MD 20878, US

[3]Faculty of Life Sciences, AV Hill Building, University of Manchester, Manchester M13 9PT, United Kingdom

[4]Division of Molecular Immunology, Medical Research Council National Institute for Medical Research, London, NW7 1AA, UK

Abstract

Enzymatically inactive chitinase-like proteins (CLPs) such as BRP-39, Ym1 and Ym2 are established markers of immune activation and pathology, yet their functions are essentially unknown. We show that Ym1 and Ym2 induce neutrophil accumulation through expansion of interleukin 17 (IL-17)-producing γδ T cells. While BRP-39 did not influence neutrophilia, it was required for IL-17 production in γδ T cells, suggesting IL-17 regulation is an inherent feature of murine CLPs. Using a model of lung migrating nematode infection, we also found that IL-17 and neutrophilic inflammation induced by Ym1 limited parasite survival but at the cost of enhanced lung injury. These studies describe effector functions of CLPs consistent with innate host defense traits of the chitinase family.

Chitinase-like proteins (CLPs) are associated with a range of different pathologies and are some of the most abundantly expressed proteins under conditions of type 2 immune activation but their functions remain poorly understood[1]. The CLPs are members of a family that include chitotriosidase and acidic mammalian chitinase (AMCase), enzymes that cleave chitin, a widespread structural component of arthropods, parasites and fungi. Consistent with

Correspondence should be sent to J.E.A. (j.allen@ed.ac.uk) or T.E.S. (tara.sutherland@ed.ac.uk). Ashworth Laboratories, Charlotte Auerbach Road, University of Edinburgh, Edinburgh EH9 3FL, UK, Phone: +44 131 650-7014, Fax: +44 131 650 5450.

AUTHOR CONTRIBUTIONS

T.E.S. designed and performed research, analyzed and interpreted data and wrote the manuscript; N.L. and V.P. performed research; D.R, A.A.H, S.M.A., V.P. and B.S. contributed vital new tools; R.M.M. contributed to data interpretation and manuscript preparation; J.E.A contributed experimental design, data interpretation and manuscript preparation.

COMPETING FINANCIAL INTERESTS

The authors declare no conflict of interest.

Europe PMC Funders Author Manuscripts

the function of chitinases throughout the evolutionary tree[1], the active chitinase enzymes act as host defense molecules against chitin-containing pathogens[2-4]. The CLPs, however, are catalytically inactive due to loss-of-function mutations[5]. Evolutionarily recent gene duplication events in mammals have resulted in expansion and diversification of the CLP genes such that each mammalian species exhibits a different array of CLP genes[5]. In mice there are three CLPs, designated Ym1, Ym2 and BRP-39, while humans have two; YKL-39 and YKL-40. The rapid divergence of CLPs in mammalian species implicates a role in host defense but their expression patterns in many non-infectious settings[1, 6] precludes defense against pathogens as the sole function.

The murine proteins, Ym1 (*Chil3*) and Ym2 (*Chil4*) were the first CLPs to be implicated as mediators of T_H2-inflammation in allergy[7,8]. Despite extensive publications that describe an increased expression of Ym1 during a wide range of pathologies, Ym1 is often disregarded as an important player in CLP biology because of the lack of a true Ym1/Ym2 human ortholog. Instead an emphasis has been placed on murine BRP-39 (*Chil1*), which has a human homologue YKL-40 (*CHIL3L1*). Recent transgenic mouse models have shown that both BRP-39 and YKL-40 can contribute to the pathology of airways disease[9-12]. Because all three murine CLPs are upregulated in response to T_H2-driven inflammation in the lungs of mice, studying BRP-39 in isolation may not reveal the true functions of this closely related protein family.

We aim to understand the general biology of CLPs by considering them as a family, rather than studying each in isolation. Our results revealed an unexpected role for Ym1 and to some extent Ym2, in driving neutrophil recruitment into the lung, due to the ability of Ym1 and Ym2 to increase the number of γδ T cells expressing IL-17A. Although BRP-39 did not significantly influence neutrophil numbers, like Ym1 and Ym2, it altered IL-17 responses in the models tested, indicating that the ability to modulate IL-17 is a key feature of all three CLPs. We further demonstrate that neutrophil recruitment observed during lung migration of *Nippostrongylus brasiliensis* is largely mediated by Ym1 in an IL-17 dependent manner. As predicted, the Ym1-induced neutrophilia contributed to acute lung damage but unexpectedly Ym1 and IL-17 impaired parasite survival. We thus highlight an anti-parasite effector mechanism by which Ym1 negatively influences the integrity of parasites through IL-17 mediated neutrophil recruitment but at a cost of increased lung damage.

Results

Ym1 is the dominant CLP in the lung

We examined the expression of *Chil1, Chil3* and *Chil4*, in the lungs of BALB/c mice during T_H2-responses that result from ovalbumin (OVA)-induced allergic airway inflammation (AAI) or innate responses that occur as a part of acute lung injury during *N. brasiliensis* infection. In the steady state, *Chil3* is the most abundant CLP, followed by *Chil1* and *Chil4* (Fig. 1a,b). Despite being barely detectable in the lungs of PBS-challenged mice (Fig. 1a), *Chil4* was up-regulated to the greatest degree after allergen challenge, followed by *Chil3* and finally *Chil4*, which showed limited change (Fig. 1a, Table 1). Similarly at day 2 post *N. brasiliensis* infection *Chil4* was the only CLP significantly upregulated, as the increase in *Chil3* and *Chil1* expression was minimal (Fig. 1b, Table 1). Despite major differences

between these models, allergy versus infection and secondary versus innate responses, the pattern of CLP expression was strikingly similar with *Chil3* the most abundant CLP, *Chil4* the most differentially regulated but least highly expressed, and *Chil1* showing the least change in its expression.

Induction of CLP gene expression was also reflected at the protein level. Due to high sequence homology between Ym1 and Ym2 (94%), there are no immunological tools that allow specific detection of Ym2 protein, rather detection antibodies recognize both Ym1 and Ym2. Protein expression of CLPs in the lung was readily detected in airway epithelial cells and macrophages following allergen challenge, with Ym1 and/or Ym2 protein up-regulated to a greater degree compared to BRP-39 (Fig. 1d). Overall our results describing gene and protein expression demonstrate that Ym1 and Ym2 are the dominant CLPs in the lungs of mice in terms of abundance and differential expression, respectively.

Ym1 over-expression results in lung neutrophilia

All CLPs exhibited increased expression during lung pathology, yet the function of these molecules, particularly Ym1 and Ym2 remains elusive. Therefore, we developed an over-expression model to assess the direct function of Ym1, Ym2 and BRP-39. Plasmids complexed to polyethylenimine (PEI) were administered intranasally to mice and transfection levels monitored by qRT-PCR. As expression peaked between 24 and 48 h (data not shown) we chose a 48 h time point for all subsequent analyses.

The number of macrophages containing microscopically observable particulate structures in mice that received plasmid directly correlated with protein expression by ELISA (data not shown), and was thus used as an indirect measure of transfection for all experiments. Approximately 35–40% of macrophages contained particulate in the bronchoalveolar lavage (BAL), independent of the plasmid administered. To confirm selective overexpression, mRNA abundance of *Chil1*, *Chil3* or *Chil4* were measured in total BAL cells. While transfection alone did not alter CLP expression (data not shown), results demonstrated specific overexpression of the relevant CLP, up to approximately 1000-fold, relative to pcDNA3.1 transfected mice ($P < 0.0001$, Fig. 2a).

Immune cell composition of the BAL and lungs was examined 48 h after plasmid administration and while administration of PEI-complexed plasmids encoding CLPs did not change total BAL or lung cells (Fig. 2b,c), neutrophil numbers were significantly increased following exogenous Ym1 expression ($P < 0.05$ compared to vector only) (Fig. 2d-f). Absolute numbers of $CD4^+$ and $CD8^+$ T cells and $CD19^+$ B cells were not altered in the lungs of transfected mice but eosinophil numbers were significantly reduced by Ym1 ($P < 0.05$ compared to vector only, Supplementary Fig. 1a-d). Thus exogenous expression of Ym1 in the lung resulted in increased numbers of neutrophils and reduced eosinophils.

Ym1 neutralization reduces neutrophilia and IL-17

We previously showed that specific inhibition of AMCase markedly increased neutrophil numbers in the lung accompanied by increased Ym1 expression[13]. Our observation that exogenous Ym1 could induce lung neutrophilia led us to speculate that the enhanced

expression of Ym1 in allergic settings may contribute to enhanced neutrophil accumulation. To test this hypothesis, we used an OVA allergen model (Supplementary Fig. 2) and a mouse monoclonal antibody raised against a peptide in the Ym1 sequence that has previously been shown to be neutralizing[14]. Although the peptide sequence is derived from Ym1, there is only 1 amino acid difference between Ym1 and Ym2 and therefore the antibody may also have activity against Ym2.

OVA-sensitized BALB/c mice were treated with anti-Ym1 or IgG2a isotype control during aerosol challenge with either PBS or OVA and BAL cell recruitment assessed (Fig. 3a). OVA-challenge increased total BAL cells and the percentage of eosinophils and neutrophils (Fig. 3b). Allergic eosinophilia remained unaffected by anti-Ym1 treatment (Fig. 3b) along with goblet cell hyperplasia and enhanced respiratory pause (penH) (data not shown). However, the percentage of neutrophils was reduced in OVA-challenged mice following treatment (Fig. 3b). This reduction was also seen in total neutrophil numbers ($1.53 \times 10^5 \pm 0.24 \times 10^5$ IgG2a treated versus $0.91 \times 10^5 \pm 0.28 \times 10^5$ anti-Ym1 treated, $P < 0.05$, Students *t*-test; mean ± s.e.m. pooled from two independent experiments of eleven to twelve mice per group).

Both innate and adaptive IL-17 production is a key process involved in promotion of neutrophil survival, recruitment and activation via regulation of target cytokine and chemokine genes[15]. Although IL-17 is more typically associated with host defense against microbial infections, an emerging role for IL-17, and indeed neutrophils, during the pathogenesis of inflammatory lung diseases, including allergy and asthma, has been highlighted over the last decade[16]. Therefore, we examined whether treatment with anti-Ym1 altered IL-17A and IL-17 target genes in allergic mice. The secretion of OVA-specific and anti-CD3-stimulated IL-17A in splenocyte cultures was increased in allergic mice, a response attenuated by anti-Ym1 treatment ($P < 0.01$ and $P < 0.05$ compared to OVA IgG2a respectively, Fig. 3c). Similarly the mRNA abundance of *Il17a* was significantly reduced in the lungs of allergic anti-Ym1 treated mice ($P < 0.05$ compared to OVA IgG2a, Fig. 3d) in addition to the IL-17 target genes and neutrophil chemotactic factors; *Cxcl5* ($P < 0.01$ compared to OVA IgG2a, Fig. 3d) and *Ccl3* ($P < 0.01$ compared to OVA IgG2a) (data not shown). Thus, the allergic lung inflammation model suggested that Ym1 regulates neutrophil numbers through changes to IL-17A and IL-17A-target genes.

γδ T cells are the source of IL-17A induced by CLPs

To test whether the effects of Ym1 and Ym2 on IL-17 were lung-specific or applied more broadly, we used the same transfection conditions as for the lung (Fig. 2) and injected plasmids encoding CLPs, control plasmid, or vehicle (5% glucose) into the peritoneal cavity. Approximately 20% of peritoneal macrophages/monocytes from transfected mice contained particulate matter corresponding to plasmid complexes and analysis of peritoneal cell mRNA abundance revealed specific overexpression of each individual CLP (Fig. 4a). Of note, Ym1 transfection increased both *Chil1* and *Chil4* mRNA expression, suggesting that CLP family members have the ability to regulate each other.

Unlike the lung transfection model, plasmid injection into the peritoneal cavity caused significant accumulation of inflammatory cells compared to glucose-injected mice (Fig. 4b).

This likely reflects the higher threshold of responsiveness to inflammatory stimuli in the lung[17]. Nonetheless, total peritoneal exudate cell (PEC) numbers following Ym1 and Ym2 transfection were higher than pcDNA3.1 control plasmid ($P < 0.05$ compared to vector; Fig. 4b). While transfection in general increased neutrophil numbers, this effect was significantly enhanced when either Ym1 or Ym2 was overexpressed (Fig. 4b). Increased neutrophil numbers were mirrored by an increase in *Il17a* expression in total PECs ($P < 0.01$ compared to vector; Fig. 4c).

To identify the source of IL-17A following Ym1 and Ym2 transfection, total PEC were stimulated *ex vivo* with the phorbol ester PMA plus ionomycin and stained intracellularly for IL-17A. Only a very small percentage of $CD4^+$ or $CD8^+$ T cells were IL-$17A^+$ (<2 % T cell population). Instead, γδ T cells constituted the major population of IL-17A producing cells (Fig. 4d) and there was no IL-17A detected in non-lymphoid cells of the peritoneal cavity. The number of interferon-γ (IFN-γ)-producing γδ T cells was not significantly altered by plasmid transfection (data not shown) but the proportion of IFN-γ^+ cells was reduced by Ym1 and Ym2 overexpression (Supplementary Fig. 3a). Of note, all CLPs increased both the total number of γδ T cells and IL-17A-producing γδ T cells compared to mice transfected with control plasmid (Fig. 4d,e). We confirmed γδ T cells were also the source of IL-17A in the lungs by transfection with Ym1 (Supplementary Fig. 3b). Both IL-1β and IL-18 can synergize with IL-23 to stimulate γδ T cells to produce IL-17A[18] and so we examined the expression of these cytokines in PECs from transfected mice. While *Il23p19* mRNA was not detected in PECs (data not shown), transfection with Ym1 and Ym2 increased the expression of both *Il1b* and *Il18* (Fig. 4f,g). BRP-39 overexpression significantly increased *Il18* abundance but not *Il1b*, potentially explaining the lack of potency of BRP-39 on IL-17A production compared to Ym1 and Ym2 (Fig. 4c,e).

Because of the very strong connection between IL-1β expression and the induction of IL-17 producing γδ T cells [18, 19], we tested whether blockade of the IL-1 receptor would alter the effect of CLPs using anakinra, an IL-1 receptor antagonist[20]. Anakinra treatment significantly reduced the ability of Ym1 to induce IL-17 producing γδ T cells (Fig. 4h and Supplementary Fig. 3c) and neutrophil accumulation (Fig. 4i) in the peritoneal cavity. Of note, anakinra also prevented suppression of IFN-γ following Ym1 overexpression (Supplemental Fig. 3d), which may contribute to the enhanced IL-17 production in the presence of Ym1. Notably, the ability to suppress IFN-γ may be a general feature of Ym1 as anti-Ym1 elevates IFN-γ production by $CD8^+$ T cells during helminth-virus coinfection[21].

Along with subsets of γδ T cells, innate lymphoid cells (ILCs) are an important source of IL-17A that promote inflammation and immunity[22, 23]. Analyzing the cellular composition of the peritoneal cavity we detected a small population of IL-$17A^+$ ILCs in both BALB/c wild-type mice and Rag2-deficient mice (Supplementary Fig. 4a,b). However, overexpression of Ym1 did not influence either the total number of ILCs or the number expressing IL-17A (Supplementary Fig. 4b). Furthermore, Ym1 failed to recruit neutrophils into the peritoneal cavity of Rag2-deficient mice (Supplementary Fig. 4c), supporting a requirement for IL-17A-expressing γδ T cells rather than ILCs. Collectively our results strongly suggest that Ym1 and Ym2 coordinate neutrophil recruitment *in vivo* by stimulating γδ T cells to produce IL-17A, via the induction of IL-1 and possibly IL-18. BRP-39 also had

the ability to influence the number of γδ T cells producing IL-17A in the peritoneal cavity (Fig. 4d,e), but this signal alone was not sufficient to significantly influence neutrophil recruitment in these models.

Ym1 contributes to *N. brasiliensis* induced lung injury

Helminth infections induce strong T_H2-type immunity. However, the initial acute response to the lung migrating nematode, *N. brasiliensis* involves tissue damage, neutrophilic inflammation and hemorrhage[24]. Previous work highlighted not only the contribution of neutrophils to nematode-induced lung damage but the role of alternatively activated macrophages in repairing that damage[24]. Since Ym1 is one of the most abundant molecules produced by macrophages in this setting, we and others have predicted its contribution to repair. However, our unexpected finding that Ym1 can induce neutrophilia, suggested that Ym1 might instead contribute to acute lung injury. To test this, BALB/c mice were infected with 500 *N. brasiliensis* infective larvae (L3s) and treated systemically with either anti-Ym1 or isotype control. The numbers of neutrophils in the BAL (Fig. 5a) and lung tissue (Fig. 5b) were pronounced at day 2 following infection and reduced by day 4. Consistent with our transfection and AAI data, treatment with anti-Ym1 prevented neutrophil influx into the airways and reduced numbers in the lung tissue at day 2 ($P < 0.01$ compared to IgG2a day 2 infected mice) (Fig. 5a,b). The numbers of BAL alveolar macrophages and lung interstitial macrophages were also reduced in infected mice at day 2 following treatment with anti-Ym1 (Fig. 5a,b), an effect that was no longer apparent at day 4, at which point mice had not received treatment for 72 h.

Changes to neutrophil numbers following anti-Ym1 treatment were mirrored by a reduction in *Il17a* (Fig. 5c) and IL-17A target chemokine genes *Cxcl5* (Fig. 5d), *Ccl3* and *Cxcl1* (data not shown) in the lung tissue of infected mice at day 2. Additionally, IL-17A secretion from splenocytes restimulated with *N. brasiliensis* excretory secretory products (NES) at day 4 post-infection were reduced by anti-Ym1 treatment, suggesting an altered adaptive IL-17 response to worm antigen (Supplementary Fig. 5a). The expression of *Il23p19* increased in the lungs following infection but was not altered by anti-Ym1 treatment (data not shown). However, as expected, *Il1b* mRNA expression in the lungs was attenuated by anti-Ym1 treatment (Fig. 5e). While the amount of IL-1β protein in whole lung homogenates was only significantly increased at day 4 post-infection of IgG2a-treated mice, anti-Ym1 reduced IL-1β abundance at day 2 ($P < 0.05$ compared to IgG2a day 2 infected mice, Fig. 5f).

We next examined whether attenuated IL-17A and reduced neutrophilia following anti-Ym1 treatment impacted on acute lung injury. Histological assessment of *N. brasiliensis* infection showed alveolar destruction and tissue hemorrhage at day 2 and the initiation of repair and accumulation of inflammatory foci by day 4 (Fig. 5g). Treatment with anti-Ym1 reduced tissue destruction observed at day 2, as also quantified by linear means intercept (L_{mi}), a measurement of airspace enlargement ($P <0.01$ compared to IgG2a day 2 infected mice, Fig. 5g). An effect of anti-Ym1 treatment was no longer evident at day 4.

If Ym1 was acting via IL-17A then IL-17A deficiency should mimic anti-Ym1 treatment during the early innate stages of infection. To test this $Il17a^{Cre}Rosa26R^{eYFP}$ mice homozygous for Cre expressing transgene replacing the endogenous *Il17a* gene and hence

deficient in IL-17A production[25], were infected with 500 *N. brasiliensis* L3 and responses at day 2 and 4 post-infection compared to C57BL/6 wild-type mice. At day 2, wild-type mice had characteristic increases in neutrophil numbers in the BAL but as expected, IL-17A-deficient mice failed to recruit neutrophils into the BAL at day 2 post-infection (Fig. 6a). Similar to previous reports regarding the role of IL-17A during acute lung injury[24, 26], IL-17A-deficient mice were protected from the peak of tissue damage following *N. brasiliensis* infection at day 2 (Fig. 6b). However, despite less initial damage in IL-17A-deficient mice, the lungs failed to repair appropriately by day 4 in comparison to wild-type mice. This may be related to our finding that in the absence of IL-17A, IL-13 was also significantly diminished (Fig. 6c). Notably, anti-Ym1 treatment also prevented this early antigen-specific IL-13 response (Supplementary Fig. 5b).

Intracellular flow cytometry for IL-17A in wild-type mice allowed us to demonstrate that as in the peritoneal cavity γδ T cells are a key source of IL-17A in the lungs of *N. brasiliensis* infected mice. Very few IL-17A$^+$ CD4$^+$ or CD8$^+$ T cells were present and rather the majority of cells expressing IL-17A were γδ T cells (Fig. 6d,e). Similar results were observed when examining eYFP expression in lung cell suspensions of infected *Il17a*^{Cre}*Rosa26R*^{eYFP} mice (Supplementary Fig. 6). Not only did we observe an increase in the number of IL-17A secreting γδ T cells, but the absolute number of all γδ T cells was increased at both day 2 and day 4 following infection (Fig. 6e). Together, the *N. brasiliensis* studies revealed that Ym1 induces IL-17A producing γδ T cells, which via IL-1 promote neutrophil accumulation and thus contribute to acute lung injury associated with larval migration in the lung.

BRP-39 regulates IL-17 expression but not neutrophilia

Although BRP-39 overexpression did not influence neutrophil numbers, it did result in enhanced IL-17A production in the peritoneal cavity and an increased number of IL-17 producing γδ T cells (Fig. 4). Because this overlapped with the observed effects of Ym1 we queried whether the CLP family may have common influences on IL-17A. *Chil1*$^{-/-}$ mice were therefore infected with *N. brasiliensis* and responses at days 2 and day 4 post-infection examined compared to C57BL/6 wild-type mice. The abundance of *Il17a* transcripts in the lung increased over the infection time course in wild-type mice as we had previously seen. In contrast, virtually no *Il17a* mRNA was detected in *Chil1*$^{-/-}$ mice at day 2 and at a much-reduced abundance at day 4 (Fig. 7a). Additionally, both the total numbers of γδ T cells and the number of γδ T cells producing IL-17A were significantly reduced in *Chil1*$^{-/-}$ animals ($P < 0.01$ D2 and $P < 0.001$ D4 compared to wild-type infected mice on respective days) (Fig. 7b). Despite these changes to IL-17A producing γδ T cells, there were no observable differences in lung neutrophil numbers (Fig. 7c), expression of *Il1b*, *Il23p19* and *Il18* (Fig. 7d), or *Cxcl5* and *Ccl3* (data not shown). Thus, not surprisingly there were no differences in tissue damage in *Chil1*$^{-/-}$ relative to wild-type mice (data not shown).

Ym1 contributes to innate anti-nematode defense

Our data demonstrate that Ym1 neutralization, neutrophil depletion or IL-17 deficiency during *N. brasiliensis* infection limit acute lung injury supported by previous studies on the roles of neutrophils and IL-17 (refs. [24, 27]). However, reduced neutrophilia and resultant

lung injury could reflect changes to numbers of larvae reaching the lung. We therefore assessed *N. brasiliensis* specific actin mRNA expression in whole lung. While this measurement cannot distinguish between live and dead larvae, it does indicate that at day 2 post-infection, at the peak of lung injury, comparable numbers of larvae have entered the lung between isotype-treated mice and anti-Ym1-treated mice (Fig. 8a), IL-17A-deficient mice (Fig. 8b) and *Chil1*$^{-/-}$ mice (Fig. 8c). Therefore, changes to neutrophilia and acute lung injury cannot be explained by a reduced number of worms reaching the lung.

Additionally worm burden was assessed in the small intestine at day 4 post-infection. Data shows anti-Ym1 treatment increased the number of larvae reaching the gut by approximately 2-fold ($P < 0.001$, Fig. 8d). IL-17A-deficient mice also exhibited increased worm burden in the small intestine at day 4 (Fig. 8e), showing a strikingly similar phenotype to Ym1 blockade (Fig. 8d). Despite reductions in IL-17A production in *Chil1*$^{-/-}$ mice, no differences in worm burden were observed (Fig. 8f) suggesting a role for neutrophils in parasite resistance. A role for neutrophils in the assault on the parasites was supported by histological analysis of neutrophils in the lungs of anti-Ym1 versus isotype treated mice (Fig. 8g). In lung sections of all mice, organized swarms of neutrophils were observed around larvae, but the number (Fig. 8h) and size (Fig. 8i) of neutrophil swarms was significantly reduced following anti-Ym1 treatment. A frequency distribution further illustrates that mice treated with anti-Ym1 not only have fewer swarms but those swarms contain only 50-100 neutrophils and do not achieve the large neutrophil numbers seen in control mice (Fig 8j). To provide further evidence that Ym1 is sufficient to enhance parasite resistance, mice were transfected with plasmid encoding Ym1 to increase protein and neutrophil numbers in the lung prior to infection with *N. brasiliensis* L3. Parasite numbers were significantly reduced in the intestines of mice that had Ym1 overexpressed in their lung (Fig 8k). Of note, the difference in parasite recovery between pcDNA3.1 control and Ym1-treated mice increased as the worms migrated through the intestine (Fig. 8l), strongly suggesting that exposure to Ym1 and neutrophils in the lung had compromised parasite fitness. Overall, the increase in gut parasite numbers demonstrates that Ym1 and IL-17A, likely through actions on neutrophils, are involved in limiting parasite burden but at the cost of enhanced lung damage.

Discussion

Neutrophils and T_H17 cells are regarded as important inflammatory cells in patients with chronic severe or steroid resistant asthma[28-30] and expression of the human CLP, YKL-40 is increased during chronic obstructive pulmonary disease[31] and active colitis[32], conditions that are also strongly associated with T_H17 and neutrophil responses (reviewed in [33, 34]). YKL-40 expression in children with severe, steroid-resistant asthma or patients with cystic fibrosis strongly correlates with neutrophil levels[11, 35], contributing to the notion that CLPs regulate neutrophilic inflammation during pathology. Our studies using direct transfection demonstrated the ability of all 3 murine CLPs to induce expansion of IL-17 producing γδ T cells. Supporting a model in which regulation of the IL-17 pathway is an inherent feature of the murine CLP family, both *Chil1*$^{-/-}$ mice and mice treated with anti-Ym1 failed to upregulate *Il17a* mRNA in the lung at day 2 following *N. brasiliensis* infection. Unlike Ym1, the influence of BRP-39 in these settings was not sufficient to influence neutrophil

numbers. Notably, our findings are consistent with studies showing a correlation between IL-17A levels and both BRP-39 and Ym1 expression[36, 37].

From an evolutionary standpoint, a role for enzymatically inactive CLPs in innate immunity is not altogether surprising considering that their close relatives contribute to immune defense by degradation of chitin from invading pathogens[38] and BRP-39 has been shown to contribute to defence against *Streptococcus pneumonia*[36]. Here we demonstrate that Ym1 and Ym2, through regulation of IL-17 producing γδ T cells and neutrophils, play a crucial host protective role by limiting nematode burden. Interestingly, a proportion of γδ T cells are similarly triggered to produce IL-17A following chitin administration in the lungs[19], but the involvement of CLPs was not explored. While control of helminth infection is typically dependent on T_H2-immunity[39], there is growing evidence that neutrophils contribute to nematode killing[40, 41]. Of note, Ym1 not only enhances neutrophil numbers in the lung at day 2 post-infection, but also alveolar and interstitial macrophages. Therefore, Ym1 may control parasite worm burden by directing both neutrophils and macrophages to damage larvae in the skin or lung before they reach the gut.

Because neutrophils and IL-17 contribute to the lung damage associated with larval migration of *N. brasiliensis*[24] we assessed the lung condition of infected mice treated with anti-Ym1. Treatment blocked neutrophil influx into both the interstitial and bronchoalveolar spaces as well as IL-17A and IL-17-driven chemokine genes in mice at day 2 post-infection. As predicted from earlier work[24], this resulted in significantly less acute lung injury, an effect mirrored in mice deficient in IL-17A. Thus, Ym1 in the early innate stages of *N. brasiliensis* promotes lung damage, presumably as a necessary consequence of limiting parasite numbers.

While the findings that a strongly T_H2-associated protein could drive neutrophil accumulation and contribute to injury responses may be somewhat surprising, Ym1 has consistently been associated with acute injury[42, 43] and indeed one of the first Ym1 publications showed rapid Ym1 expression following a stab-wound in the brain[44]. These data, along with the ability of Ym1 and Ym2 to upregulate IL-1β and early responder γδ T cells, implicate Ym1 and Ym2 as Danger-associated molecular patterns (DAMPs) that form part of the innate immune response to trauma[45]. The possibility that CLPs act as DAMPs is supported by the finding that the induction of IL-17 and neutrophils is dependent on IL-1 signaling. Although Ym1 can induce IL-1 release from peritoneal cells *in vitro*, the amount is far below that observed with well-known inflammasome activators (data not shown). We thus suspect that Ym1 is interacting with other components *in vivo*, or is triggering IL-1 release from other sources, such as epithelial cells or platelets. CLPs are lectins that can bind extracellular matrix (ECM) and cell surface heparan sulfate[46] and this may contribute to IL-1 release via receptor cross-linking, or displacement of ECM bound inflammasome mediators. Additionally Ym1 has the propensity to form crystals in pathological conditions[47], which may directly activate the inflammasome *in vivo* but not under our *in vitro* conditions. These will be important avenues for further investigation along with a specific assessment of the contribution of IL-1α versus IL-1β, and the potential role IL-18, as well as suppressed IFN-γ production.

Despite its contribution to neutrophil mediated injury, a role for Ym1 in subsequent repair would be predicted from its very abundant production by IL-4–activated macrophages[48, 49], and indeed this may be the case. At approximately day 4 post-infection with *N. brasiliensis*, the immune response starts to switch to an adaptive one, with an increase in T_H2-cytokine expression[24, 50], required for worm expulsion[51]. Repair of lung damage from larval migration also requires a competent host adaptive response[52] and IL-4Rα signaling[24] as well as an intact ILC2 population[53]. Notably, the chitin-driven γδ T cell response recently reported was dampened by activated ILC2s[19]. We saw no change in ILCs in the short time frame of the *N. brasiliensis* infections, but considering that chitin is a structural component of many pathogens including helminths, the ability to restrain excessive γδ T cell stimulation and the ensuing neutrophilic inflammation would be necessary to limit damage to the host. Indeed, our data suggest that IL-17 itself can promote the protective type 2 response as IL-17A-deficient mice showed diminished type 2 cytokine responses and there appeared to be defects in lung repair at day 4. The idea that IL-17 can promote type 2 responses in the lung is not new and has previously been reported[54-56]. While our study has focused on the early innate events, further investigation would be required to determine whether the Ym1, Ym2 or even BRP-39 mediated induction of IL-17A contributes to later repair responses.

Chromosomal location of CLPs, suggests that murine and human CLPs are derived from duplication and mutation of the active chitinases[5]. Thus, despite the differences between species, CLPs as a family are likely to share common features. Unraveling why CLP proteins are undergoing such rapid divergence is an important challenge for understanding their function relative to their non-mutating enzymatically active relatives. Our studies define a new role for CLPs in innate immune defense against nematodes. In summary, we find that murine CLPs promote IL-17 responses and that Ym1 leads to enhanced neutrophil recruitment. The consequence of Ym1 function for infection with a lung-migrating nematode, was better parasite control but at the cost of increased acute lung damage (Supplementary Fig. 7).

Methods

Mice

Wild-type (WT; BALB/c or C57BL/6), BALB/c *Rag2*$^{-/-}$, C57BL/6 *Chil1*$^{-/-}$[9] and C57BL/6 *Il17a*^{Cre}*Rosa26R*^{eYFP}[25] mice were bred in house. Mice were 7–12-weeks old at the start of the experiment and all mice were housed in individually ventilated cages. Mice were not randomized within cages, but each cage was randomly assigned to a treatment group. Investigators were not blinded to mouse identity during necropsy. Experiments were performed in accordance with the United Kingdom Animals (Scientific Procedures) Act of 1986. All experiments were performed on female mice, except for WT vs. *Il17a*^{Cre}*Rosa26R*^{eYFP} and anakinra experiments (Figs. 4,6), which were mixed sex. Sample size was calculated based on the number of animals needed to detect a 25% change in neutrophil numbers at $P < 0.05$, based on previous experiments[13].

Anti-Ym1

An anti-Ym1 mouse hybridoma cell line 4D10 was generated by immunizing mice with a Ym1 peptide (IPRLLLTSTGAGIID) conjugated to KLH and was previously shown to be neutralizing[14]. Neutralizing activity of the monoclonal antibody was verified *in vitro*. The hybridoma cell line 2D12 was purchased from the European Collection of Cell Cultures was used as an IgG2a isotype control antibody. Secreted antibodies were purified using protein G affinity chromatography.

Plasmids

The full-length-coding region of murine *Chil1*, *Chil3* and *Chil4* were amplified using a mouse lung cDNA template. The cDNA fragments were directionally cloned into pcDNA3.1 (Invitrogen) to generate plasmids encoding V5/His tagged CLPs. TOP10 competent cells were transformed with CLP plasmids or pcDNA3.1 and sequence confirmed. Plasmids were routinely grown in transformed using JM109 cells (Promega) and plasmids isolated with miniprep kits (Qiagen) before undergoing endotoxin removal (MiraCLEAN Kit, Mirus) and plasmid concentration. DNA concentration was quantified by fluorometric methods (Qubit, Life Technologies).

In vivo transfection

pcDNA3.1 plasmid (control) or plasmids encoding BRP-39, Ym1 or Ym2 were complexed with in vivo JetPEI (Polyplus Transfection) at an N:P ratio (number of nitrogen residues of jetPEI per DNA phosphate) of 8. Complexes were administered to mice at a dose 20 μg of plasmid, either via intranasal or intraperitoneal route. The bronchoalveolar lavage (BAL) and lungs, or PEC were harvested 48 h after transfection. Mice that were not transfected were excluded from the analysis.

IL-1 receptor blockade

BALB/c WT mice received two intraperitoneal doses of 100 mg/kg human-IL-1Ra (r-met-huIL-1RA:Kineret; Amgen) or PBS vehicle 4 and 24 h post transfection with pcDNA3.1 or plasmid encoding Ym1 (20 μg, i.p.).

Allergic inflammation

Allergic airway inflammation (AAI) was induced in mice in a similar manner as previously described[13]. Briefly, BALB/c mice were sensitized (day 0) with 20 μg OVA precipitated with alum, i.p. prior to 30 min aerosol challenges with PBS or 1 % OVA on days 8, 9 and 10 (Fig. 3a). Mice were treated with 200 μg anti-Ym1 or IgG2a isotype control antibody intraperitoneally 1 day prior to challenge and everyday thereafter. On day 11, BAL was performed and lungs taken for further assays and analysis.

Nippostrongylus brasiliensis infection

N. brasiliensis was maintained by serial passage through Sprague-Dawley rats, as described previously[57]. Third-stage larvae (L3's) were washed 10x with sterile PBS prior to infection. On day 0, BALB/c WT mice were infected with 500 (L3's) subcutaneously, treatment with 200 μg of anti-Ym1 or isotype control (intraperitoneally) occurred on day −1, 0 and 1.

Additionally, C57BL/6 WT, C57BL/6 *Chil1*$^{-/-}$ or *Il17a*^{Cre}*Rosa26R*^{eYFP} were infected with 500 L3's subcutaneously on day 0. On day 2 and day 4, BAL was performed and lungs taken for further assays and analysis. Single cell suspensions of splenocytes were restimulated *ex vivo* with NES antigen[58] (1 μg/mL) or anti-CD3 (1 μg/mL). Cell supernatants were harvested 72 h later and stored at −20°C until further analysis. BALB/c WT mice were also transfected with pcDNA3.1 or a plasmid encoding Ym1 (20 μg, i.n.) one day prior to infection with 500 L3's subcutaneously. On day 4 post-infection, the small intestines from infected mice were collected in D-PBS (Sigma) and the numbers of worms counted.

Histology and immunofluorescence

Cytospins were prepared from BAL cells and stained with Kwik-Diff (Thermo Scientific). Lung tissue was fixed perfused with 10 % neutral buffered formalin (Sigma) and incubated overnight before being transferred to 70 % ethanol. Lungs were paraffin-embedded, sectioned and stained for H&E. Linear means intercept (L_{mi}) method was used to quantify emphysema like damage[59]. To calculate L_{mi}, 15 random non-overlapping fields (magnification ×200) per H&E stained lung sample were taken. Six horizontal lines were drawn across each image (ImageJ 1.44) and the total number of alveolar wall intercepts counted per line. The length of each line was then divided by the number of intercepts to give the L_{mi}. Images that included large bronchi and vessels were avoided and analysis was performed in a blinded and randomized fashion. For immunofluorescence imaging, lung sections were deparaffinized and incubated in Dako Target Retrieval Solution, pH 9.0 (S2368) at 97 °C for 45 min to retrieve antigen and stained with a rabbit polyclonal antibody against myeloperoxidase (1:200 in 2% BSA, 2% donkey serum, Dako GA511) and DAPI to stain DNA, to study patterns of neutrophil recruitment. Swarms were identified by analysis of MPO labeled images in ImageJ. A binary image was created using the threshold function to mark individual cells, a Voronoi binary analysis was applied and subsequently inverted. This image was then analyzed by filtering out large Voronoi tiles using upper area limits to create a mask with regions of interest that covered lung areas containing closely clustered neutrophils. Adjacent tiles were clustered into a single swarm. These masks were also applied to the original images of individual cells to obtain the number of neutrophils within each cluster.

RNA extraction and quantitative real-time PCR

A section of the right lung lobe was stored in RNAlater (Ambion) prior to homogenising tissue in Trifast GOLD (Peqlab) with a TissueLyser (Qiagen) and RNA was prepared according to manufacturer's instructions. Reverse transcription was performed using 0.25-1.00 μg of total RNA using 50 U Tetro reverse transcriptase (Bioline), 40 mM dNTPs (Promega), and 0.5 μg Oligo dT15 (Roche) and RNasin inhibitor (Promega). Transcript abundance of genes of interest were measured by real-time PCR with the Lightcycler 480 II system (Roche) using SYBR Green I Master kit and specific primer pairs (Supplementary Table 1) as previously described[13]. PCR amplification was analyzed using 2nd derivative maximum algorithm (LightCycler 480 Sw 1.5, Roche) and the expression of the gene of interest was normalized to a housekeeping gene *Rpl13a*.

Flow cytometry

Single cell suspensions from right lung lobe was prepared by digesting with 0.2 U/mL Liberase TL (Roche) and 80 U/mL DNase (Life Tech) in HBSS at 37 °C for 25 m, followed by forcing tissue suspensions through gauze. Red blood cells (RBCs) were lysed (Sigma) and total cells counted using a Scharf Instruments cell counter (Roche) or an automated cellometer T4 (Peqlab). Cells were incubated with Fc block (CD16/CD32 and mouse serum) and stained with fluorescent conjugated antibodies to CD11b (M1/70), CD11c (N418), F4/80 (BM8), Ly6G (1A8), CD4 (GK1.5), CD8 (52-6.7), TCRγδ (GL3), CD90.2 (30-H12), CD25 (PC61), CD127 (A7R34), (Biolegend), I-A/I-E (MHCII) (M5/114.15.2), CD19 (6D5), TCRβ (H57-597) (eBioscience) and Siglec F (E50-2440) (BD Biosciences). Cells were identified by the following surface markers: neutrophils were $CD11b^+$ $Ly6G^+$ $F4/80^-$; interstitial lung macrophages were $F4/80^+$ $CD11b^+$ $CD11c^-$ $SigF^-$; γδ T cells were $TCR\gamma\delta^+$ $TCR\beta^-$ $CD4^-$ $CD8^-$ $CD11b^-$; and innate lymphoid cells (ILCs) were lineage negative (CD3, CD19, F4/80, SigF, Ly6G, CD11c, CD11b, TER119), $CD90.2^+$ $CD25^+$ $CD127^+$. Cells were fixed with 2 % paraformaldehyde for 10 min at 20 °C and stored at 4 °C until stained intracellularly or acquired. Where intracellular staining for IL-17A was performed, cells were stimulated for 4 h at 37 °C with phorbol myristate acetate (PMA; 0.5 μg/ml), ionomycin (1 μg/ml) and for 3 h at 37 °C with Brefaldin A (10 μg/ml) (Sigma). Cells were surfaced stained and fixed with 2 % paraformaldehyde, then permeabilized according to manufacturer's instructions (eBioscience) and stained with APC anti-mouse IL-17A (TC11-18H10.1) or APC anti-mouse IgG1 isotype control (MOPC-21) and F488 anti-mouse IFNγ (XMG1.2) or F488 anti-mouse IgG1 isotype control (MOPC-21) (Biolegend), prior to acquisition. Live/dead aqua (Life Technologies) was used to exclude dead cells from analysis. Samples were analysed by flow cytometry using Becton-Dickinson FACS Canto II or LSR II and cells were characterised using FlowJo software.

Quantification of cytokines

Mouse IL-17 and IL-13 Duo-Set ELISA (R&D Systems) were used for the measurement of IL-17A and IL-13 in thoracic lymph node or splenocyte culture supernatants following stimulation with OVA or *N. brasiliensis* excretory secretory (NES) antigens or anti-CD3 mitogen for 72 h. Whole lung tissue was homogenized in Hanks' balanced salt solution containing protease inhibitor cocktail (Sigma). Protein concentrations of IL-1β were measured in homogenate supernatant by ELISA (eBioscience).

Statistical analysis

Statistical analysis was performed with JMP statistical analysis software (JMP 11; SAS Institute Inc). Normal distribution of data was determined by optical examination of residuals and each group was tested for unequal variances using Welch's test. Differences between groups were determined by analysis of variance (ANOVA) followed by a Tukey-Kramer HSD multiple comparison test or unpaired two-tailed Student's *t*-test as indicated. In some cases, data were log-transformed to achieve normal distribution. However, in situations when this was not possible, a Kruskal-Wallis test was used. Differences were considered statistically significant for *P* values of less than 0.05.

Supplementary Material

Refer to Web version on PubMed Central for supplementary material.

ACKNOWLEDGMENTS

The authors thank S. Duncan and Y. Harcus for excellent technical assistance and R. Zamoyska for helpful discussion. This work was funded by the Medical Research Council United Kingdom (MRC-UK MR/J001929/1 and MC_UP_1202/13 for V.P.) and Asthma UK (06/057 & 10/040) with support from the Wellcome Trust funded Centre for Immunity, Infection and Evolution.

The funders had no role in study design, data collection and analysis, decision to publish, or preparation of the manuscript.

References

1. Sutherland TE, Maizels RM, Allen JE. Chitinases and chitinase-like proteins: potential therapeutic targets for the treatment of T-helper type 2 allergies. Clin. Exp. Allergy. 2009; 39:943–955. [PubMed: 19400900]
2. Labadaridis I, et al. Chitotriosidase in neonates with fungal and bacterial infections. Arch. Dis. Child Fetal Neonatal Ed. 2005; 90:F531–532. [PubMed: 16244214]
3. Barone R, et al. Plasma chitotriosidase activity in acute Plasmodium falciparum malaria. Clin. Chim. Acta. 2003; 331:79–85. [PubMed: 12691867]
4. Nance JP, et al. Chitinase dependent control of protozoan cyst burden in the brain. PLoS Pathog. 2012; 8:e1002990. [PubMed: 23209401]
5. Bussink AP, Speijer D, Aerts JM, Boot RG. Evolution of mammalian chitinase(-like) members of family 18 glycosyl hydrolases. Genetics. 2007; 177:959–970. [PubMed: 17720922]
6. Lee CG, et al. Role of chitin and chitinase/chitinase-like proteins in inflammation, tissue remodeling, and injury. Annu. Rev. Physiol. 2011; 73:479–501. [PubMed: 21054166]
7. Webb DC, McKenzie AN, Foster PS. Expression of the Ym2 lectin-binding protein is dependent on interleukin (IL)-4 and IL-13 signal transduction: identification of a novel allergy-associated protein. J Biol Chem. 2001; 276:41969–41976. [PubMed: 11553626]
8. Welch JS, et al. TH2 cytokines and allergic challenge induce Ym1 expression in macrophages by a STAT6-dependent mechanism. J Biol Chem. 2002; 277:42821–42829. [PubMed: 12215441]
9. Lee CG, et al. Role of breast regression protein 39 (BRP-39)/chitinase 3-like-1 in Th2 and IL-13-induced tissue responses and apoptosis. J. Exp. Med. 2009; 206:1149–1166. [PubMed: 19414556]
10. Sohn MH, et al. The chitinase-like proteins breast regression protein-39 and YKL-40 regulate hyperoxia-induced acute lung injury. Am. J. Respir. Crit. Care. Med. 2010; 182:918–928. [PubMed: 20558631]
11. Hector A, et al. The chitinase-like protein YKL-40 modulates cystic fibrosis lung disease. PLoS One. 2011; 6:e24399. [PubMed: 21949714]
12. Nikota JK, et al. Differential expression and function of breast regression protein 39 (BRP-39) in murine models of subacute cigarette smoke exposure and allergic airway inflammation. Respir. Res. 2011; 12:39. [PubMed: 21473774]
13. Sutherland TE, et al. Analyzing airway inflammation with chemical biology: dissection of acidic mammalian chitinase function with a selective drug-like inhibitor. Chem. Biol. 2011; 18:569–579. [PubMed: 21609838]
14. Arora M, et al. Simvastatin promotes Th2-type responses through the induction of the chitinase family member Ym1 in dendritic cells. Proc. Natl. Acad. Sci. U S A. 2006; 103:7777–7782. [PubMed: 16682645]
15. Ye P, et al. Requirement of interleukin 17 receptor signaling for lung CXC chemokine and granulocyte colony-stimulating factor expression, neutrophil recruitment, and host defense. J. Exp. Med. 2001; 194:519–527. [PubMed: 11514607]

16. Aujla SJ, Alcorn JF. T(H)17 cells in asthma and inflammation. Biochim. Biophys. Acta. 2011; 1810:1066–1079. [PubMed: 21315804]
17. Raz E. Organ-specific regulation of innate immunity. Nat. Immunol. 2007; 8:3–4. [PubMed: 17179960]
18. Lalor SJ, et al. Caspase-1-processed cytokines IL-1beta and IL-18 promote IL-17 production by gammadelta and CD4 T cells that mediate autoimmunity. J. Immunol. 2011; 186:5738–5748. [PubMed: 21471445]
19. Van Dyken SJ, et al. Chitin Activates Parallel Immune Modules that Direct Distinct Inflammatory Responses via Innate Lymphoid Type 2 and gammadelta T Cells. Immunity. 2014; 40:414–424. [PubMed: 24631157]
20. Nielsen MM, et al. IL-1beta-dependent activation of dendritic epidermal T cells in contact hypersensitivity. J. Immunol. 2014; 192:2975–2983. [PubMed: 24600030]
21. Osborne LC, et al. Coinfection. Virus-helminth coinfection reveals a microbiota-independent mechanism of immunomodulation. Science. 2014; 345:578–582. [PubMed: 25082704]
22. Gladiator A, Wangler N, Trautwein-Weidner K, LeibundGut-Landmann S. Cutting edge: IL-17-secreting innate lymphoid cells are essential for host defense against fungal infection. J. Immunol. 2013; 190:521–525. [PubMed: 23255360]
23. Kim HY, et al. Interleukin-17-producing innate lymphoid cells and the NLRP3 inflammasome facilitate obesity-associated airway hyperreactivity. Nat. Med. 2014; 20:54–61. [PubMed: 24336249]
24. Chen F, et al. An essential role for TH2-type responses in limiting acute tissue damage during experimental helminth infection. Nat. Med. 2012; 18:260–266. [PubMed: 22245779]
25. Hirota K, et al. Fate mapping of IL-17-producing T cells in inflammatory responses. Nat. Immunol. 2011; 12:255–263. [PubMed: 21278737]
26. Li C, et al. IL-17 response mediates acute lung injury induced by the 2009 pandemic influenza A (H1N1) virus. Cell Res. 2012; 22:528–538. [PubMed: 22025253]
27. Grommes J, Soehnlein O. Contribution of neutrophils to acute lung injury. Mol. Med. 2011; 17:293–307. [PubMed: 21046059]
28. The ENFUMOSA cross-sectional European multicentre study of the clinical phenotype of chronic severe asthma. European Network for Understanding Mechanisms of Severe Asthma. Eur. Respir. J. 2003; 22:470–477. [PubMed: 14516137]
29. Al-Ramli W, et al. T(H)17-associated cytokines (IL-17A and IL-17F) in severe asthma. J. Allergy Clin. Immunol. 2009; 123:1185–1187. [PubMed: 19361847]
30. Newcomb DC, Peebles RS Jr. Th17-mediated inflammation in asthma. Curr. Opin. Immunol. 2013; 25:755–760. [PubMed: 24035139]
31. Letuve S, et al. YKL-40 is elevated in patients with chronic obstructive pulmonary disease and activates alveolar macrophages. J. Immunol. 2008; 181:5167–5173. [PubMed: 18802121]
32. Vind I, Johansen JS, Price PA, Munkholm P. Serum YKL-40, a potential new marker of disease activity in patients with inflammatory bowel disease. Scand. J. Gastroenterol. 2003; 38:599–605. [PubMed: 12825867]
33. Alcorn JF, Crowe CR, Kolls JK. TH17 cells in asthma and COPD. Annu. Rev. Physiol. 2010; 72:495–516. [PubMed: 20148686]
34. Morrison PJ, Ballantyne SJ, Kullberg MC. Interleukin-23 and T helper 17-type responses in intestinal inflammation: from cytokines to T-cell plasticity. Immunology. 2011; 133:397–408. [PubMed: 21631495]
35. Konradsen JR, et al. The chitinase-like protein YKL-40: A possible biomarker of inflammation and airway remodeling in severe pediatric asthma. J. Allergy Clin. Immunol. 2013
36. Dela Cruz CS, et al. Chitinase 3-like-1 promotes Streptococcus pneumoniae killing and augments host tolerance to lung antibacterial responses. Cell Host Microbe. 2012; 12:34–46. [PubMed: 22817986]
37. Sakazaki Y, et al. Overexpression of chitinase 3-like 1/YKL-40 in lung-specific IL-18-transgenic mice, smokers and COPD. PLoS One. 2011; 6:e24177. [PubMed: 21915293]

38. Tran HT, Barnich N, Mizoguchi E. Potential role of chitinases and chitin-binding proteins in host-microbial interactions during the development of intestinal inflammation. Histol. Histopathol. 2011; 26:1453–1464. [PubMed: 21938682]
39. Anthony RM, et al. Protective immune mechanisms in helminth infection. Nat. Rev. Immunol. 2007; 7:975–987. [PubMed: 18007680]
40. Bonne-Annee S, et al. Human and mouse macrophages collaborate with neutrophils to kill larval Strongyloides stercoralis. Infect. Immun. 2013; 81:3346–3355. [PubMed: 23798541]
41. O'Connell AE, et al. Major basic protein from eosinophils and myeloperoxidase from neutrophils are required for protective immunity to Strongyloides stercoralis in mice. Infect. Immun. 2011; 79:2770–2778. [PubMed: 21482685]
42. Loke P, et al. Alternative activation is an innate response to injury that requires CD4+ T cells to be sustained during chronic infection. J. Immunol. 2007; 179:3926–3936. [PubMed: 17785830]
43. Ydens E, et al. Acute injury in the peripheral nervous system triggers an alternative macrophage response. J. Neuroinflammation. 2012; 9:176. [PubMed: 22818207]
44. Hung SI, Chang AC, Kato I, Chang NC. Transient expression of Ym1, a heparin-binding lectin, during developmental hematopoiesis and inflammation. J. Leukoc. Biol. 2002; 72:72–82. [PubMed: 12101265]
45. Pittman K, Kubes P. Damage-associated molecular patterns control neutrophil recruitment. J. Innate. Immun. 2013; 5:315–323. [PubMed: 23486162]
46. Prakash M, et al. Diverse pathological implications of YKL-40: answers may lie in 'outside-in' signaling. Cellular signalling. 2013; 25:1567–1573. [PubMed: 23562456]
47. Guo L, Johnson RS, Schuh JC. Biochemical characterization of endogenously formed eosinophilic crystals in the lungs of mice. J Biol Chem. 2000; 275:8032–8037. [PubMed: 10713123]
48. Falcone FH, et al. A Brugia malayi homolog of macrophage migration inhibitory factor reveals an important link between macrophages and eosinophil recruitment during nematode infection. J. Immunol. 2001; 167:5348–5354. [PubMed: 11673551]
49. Loke P, et al. IL-4 dependent alternatively-activated macrophages have a distinctive in vivo gene expression phenotype. BMC Immunol. 2002; 3:7. [PubMed: 12098359]
50. Voehringer D, Shinkai K, Locksley RM. Type 2 immunity reflects orchestrated recruitment of cells committed to IL-4 production. Immunity. 2004; 20:267–277. [PubMed: 15030771]
51. Urban JF Jr. et al. IL-13, IL-4Ralpha, and Stat6 are required for the expulsion of the gastrointestinal nematode parasite Nippostrongylus brasiliensis. Immunity. 1998; 8:255–264. [PubMed: 9492006]
52. Reece JJ, Siracusa MC, Scott AL. Innate immune responses to lung-stage helminth infection induce alternatively activated alveolar macrophages. Infect. Immun. 2006; 74:4970–4981. [PubMed: 16926388]
53. Turner JE, et al. IL-9-mediated survival of type 2 innate lymphoid cells promotes damage control in helminth-induced lung inflammation. J. Exp. Med. 2013; 210:2951–2965. [PubMed: 24249111]
54. Kallal LE, et al. Inefficient lymph node sensitization during respiratory viral infection promotes IL-17-mediated lung pathology. J. Immunol. 2010; 185:4137–4147. [PubMed: 20805422]
55. Lajoie S, et al. Complement-mediated regulation of the IL-17A axis is a central genetic determinant of the severity of experimental allergic asthma. Nat. Immunol. 2010; 11:928–935. [PubMed: 20802484]
56. Wang M, et al. Immunomodulatory effects of IL-23 and IL-17 in a mouse model of allergic rhinitis. Clin. Exp. Allergy. 2013; 43:956–966. [PubMed: 23889249]
57. Lawrence RA, Gray CA, Osborne J, Maizels RM. Nippostrongylus brasiliensis: cytokine responses and nematode expulsion in normal and IL-4-deficient mice. Exp. Parasitol. 1996; 84:65–73. [PubMed: 8888733]
58. Holland MJ, Harcus YM, Riches PL, Maizels RM. Proteins secreted by the parasitic nematode Nippostrongylus brasiliensis act as adjuvants for Th2 responses. Eur. J. Immunol. 2000; 30:1977–1987. [PubMed: 10940887]
59. Thurlbeck WM. Measurement of pulmonary emphysema. The American review of respiratory disease. 1967; 95:752–764. [PubMed: 5337140]

Europe PMC Funders Author Manuscripts

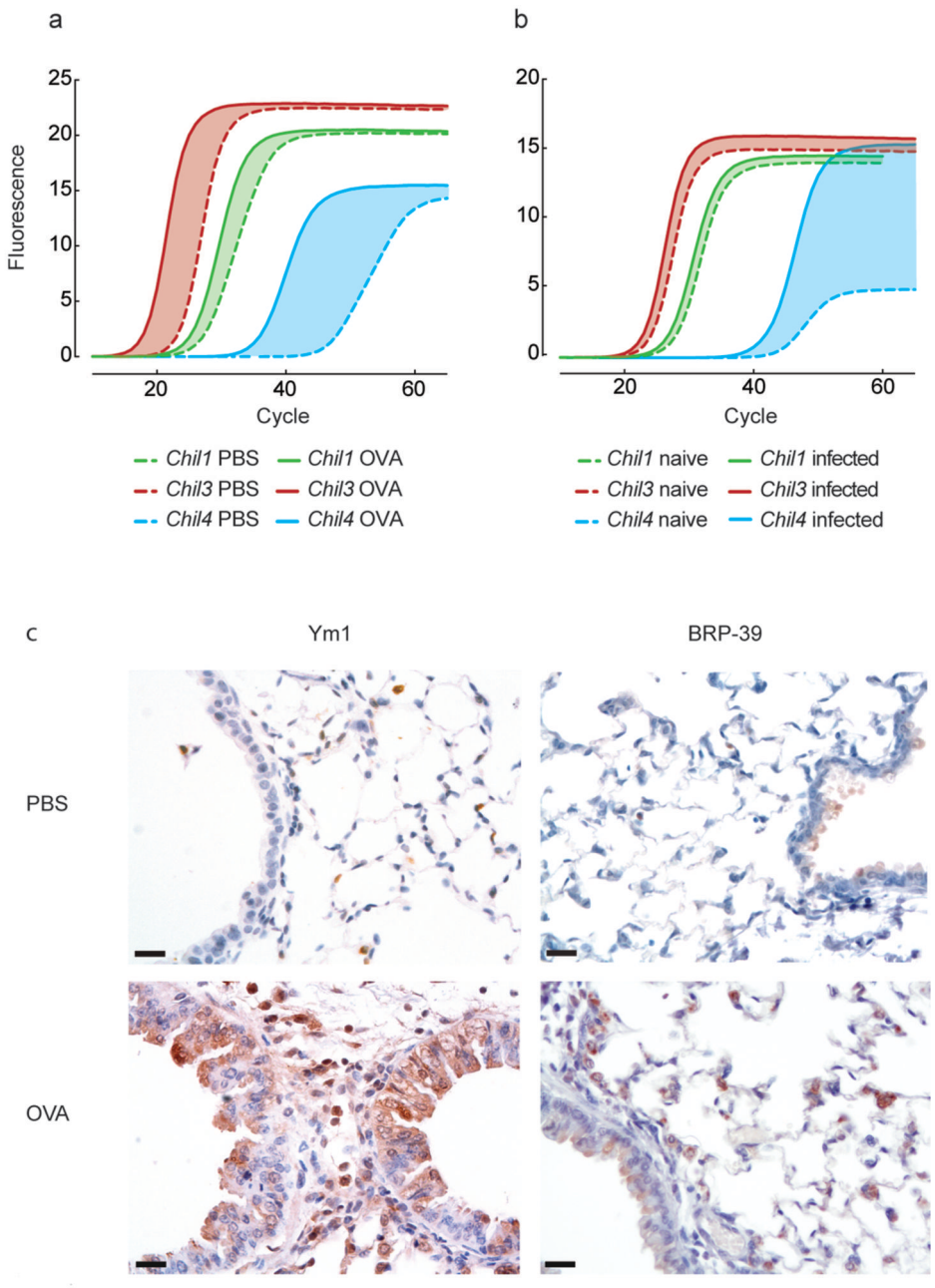

Figure 1. The expression of CLPs in the lungs of mice

(a-b) mRNA amplification in lung tissue from PBS or OVA-challenged BALB/c mice (**a**) or uninfected or *N. brasiliensis* infected BALB/c mice (day 2 after infection) (**b**). Graphs show mean SYBR green fluorescence over cycle number with cycle number reflecting the relative abundance of the gene and the shaded area between the curves reflecting mean up-regulation of each gene. (**c**) Anti-Ym1 or anti-BRP-39 stained lung sections from PBS- or OVA-challenged mice. Scale bar, 20 μm. Data are representative of three independent experiments.

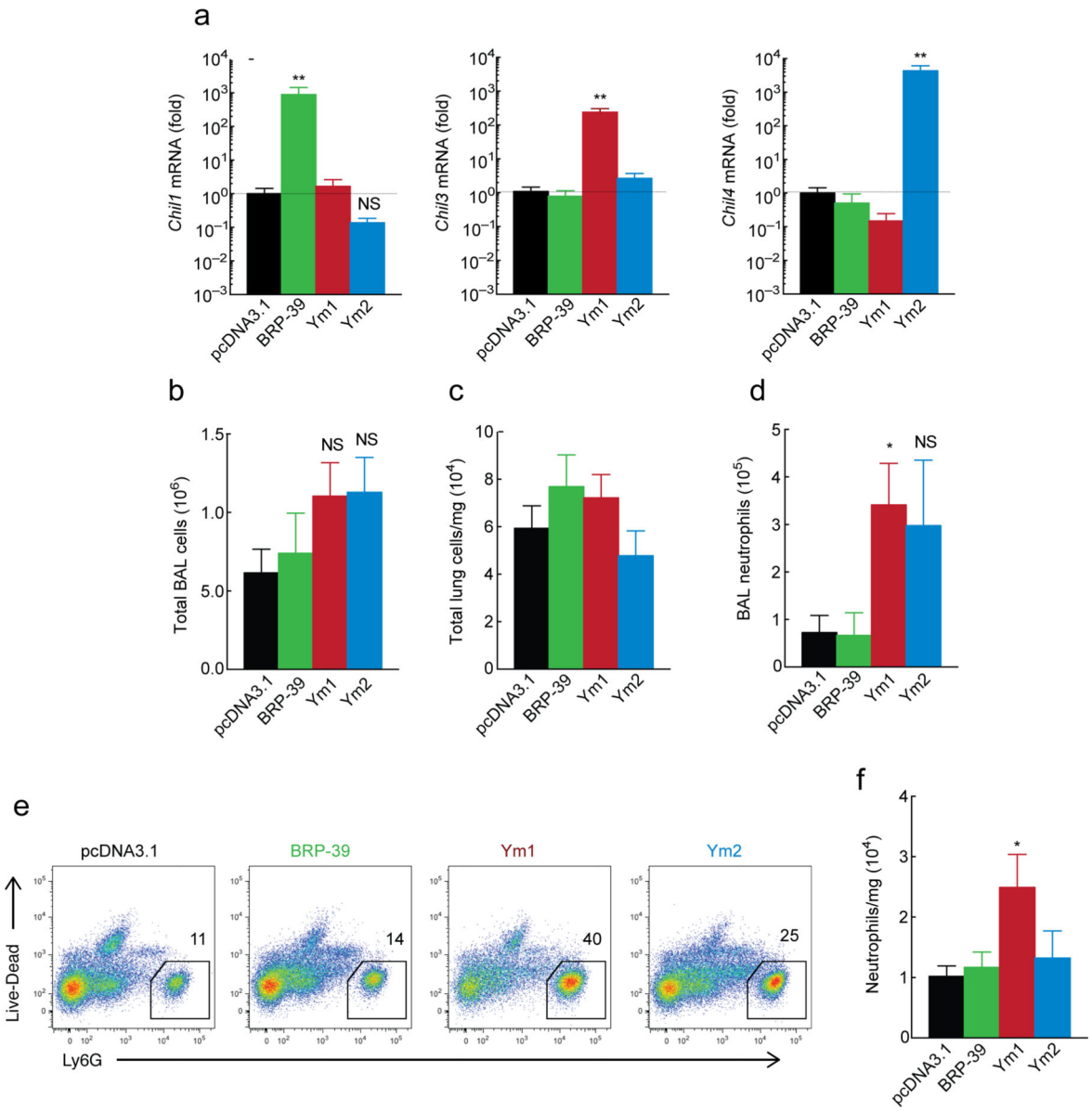

Figure 2. Over-expression of Ym1 in the lungs induces neutrophil accumulation

(**a**) Gene expression in total BAL cells from mice 48 h after intranasal transfection with 20 μg pcDNA3.1 or plasmids encoding BRP-39, Ym1 or Ym2, shown as the fold increase over pcDNA3.1. (**b-c**) Absolute number of total BAL cells (**b**) and total lung cells/mg tissue (**c**) from mice as in **a**. (**d**) Absolute numbers of BAL neutrophils as identified from DiffQuick stained cytospins from mice as in **a**. (**e**) Expression of Ly6G by single cell lung suspensions from mice as in a. Numbers above outlined area indicate percentages of $Ly6G^+$ $CD11b^+$ neutrophils. (**f**) Absolute numbers of neutrophils in the lungs of mice, normalized to lung weight as identified from mice as in **e**. **P* <0.05, ***P* <0.0001 and NS not significant compared to pcDNA3.1 transfected mice (analysis of variance with (**a**) Tukey-Kramer HSD multiple comparison test or (**b,d,f**) Kruskal-Wallis post-hoc test). Data are pooled (**a-d, f**;

mean ± s.e.m) or representative (**e**) from two individual experiments with five to nine mice per group.

Europe PMC Funders Author Manuscripts

Europe PMC Funders Author Manuscripts

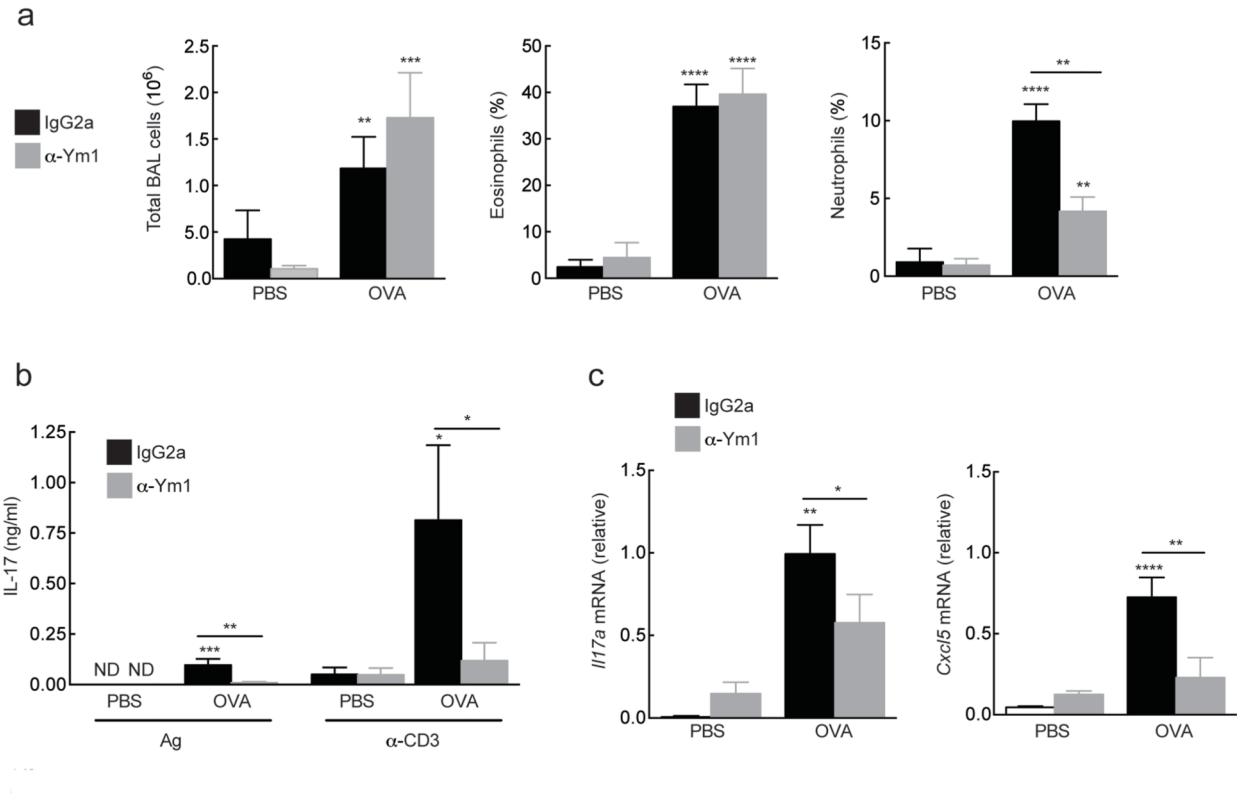

Figure 3. Ym1 promotes OVA-induced neutrophilia and regulates IL-17A abundance

(**a-c**) Cells from BAL of PBS or OVA-challenged mice treated with IgG2a or anti-Ym1 (200 μg, i.p.). showing total numbers and percentage of eosinophils and neutrophils as calculated from DiffQuick stained cytospins. (**b**) IL-17A secreted from thoracic lymph node cells cultured with OVA antigen (Ag, 500 μg) or α-CD3 (1 μg/mL) from mice as in **a**. Data show IL-17A responses normalized to amount of IL-17A secreted in medium controls for each individual mouse. (**c**) Gene expression in lung tissue of mice as in **a**. ND, not detected. **P* < 0.05, ***P* < 0.01, ****P* < 0.001 and *****P* < 0.0001 (analysis of variance with (**a, d**) Tukey-Kramer HSD multiple comparison test or (**c**) Kruskal-Wallis test). Data are pooled (**a**; mean ± s.e.m.) or representative (**c**, **d**; mean ± s.e.m.) from two independent experiments of eleven to twelve mice per group.

Europe PMC Funders Author Manuscripts

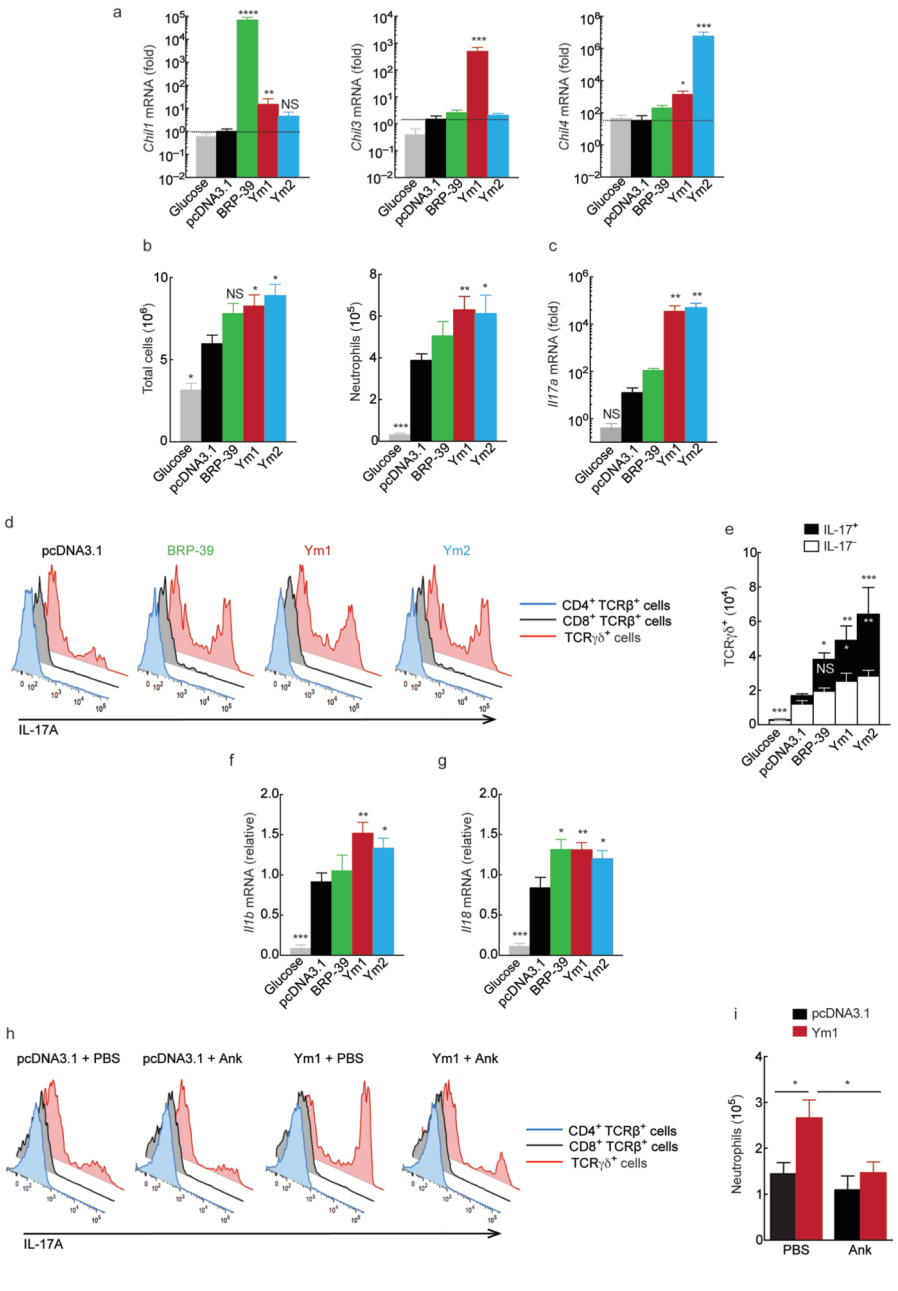

Figure 4. CLPs alter neutrophil recruitment in the peritoneal cavity

(**a**) Gene expression in PEC collected at 48 h from mice administered with pCDNA3.1, plasmids encoding BRP-39, Ym1 or Ym2 (20 μg) or glucose (i.p.). Data show fold change over pcDNA3.1. (**b**) Absolute numbers of viable cells and Ly6G$^+$ Cd11b$^+$ F4/80$^-$ neutrophils in PEC from mice as in **a**. (**c**) Relative gene expression in PEC from mice as in **a**. (**d**) Expression of IL-17A in PMA and ionomycin restimulated PEC from mice as in **a**. (**e**) Absolute number of IL-17$^-$ or IL-17$^+$ TCRγδ cells from mice as in **a**. Statistics depicts significance of IL-17A$^+$ γδ T cells in black, and total γδ T cells in white. (**f**-**g**) Relative gene expression in PEC from mice as in **a**. (**h**) Expression of IL-17A in PMA and ionomycin

restimulated PEC from mice collected 48 h after intraperitoneal transfection with pcDNA3.1 or a plasmid encoding Ym1 and treated with 100 mg/kg anakinra (Ank) or PBS (i.p.). (**i**) Absolute numbers of neutrophils in PEC from mice as in **h** and analysed as in **b**. NS not significant; *$P < 0.05$; **$P < 0.01$; ***$P < 0.001$ and ****$P < 0.0001$ compared to pcDNA3.1 transfected mice (analysis of variance with Tukey-Kramer HSD multiple comparison test). Data are pooled from two independent experiments with eight to eleven mice per group (**a-c, e-g;** mean ± s.e.m) or are representative of two independent experiments with five to seven mice per group (**d**, **h-i;** mean ± s.e.m. in **i**).

Europe PMC Funders Author Manuscripts

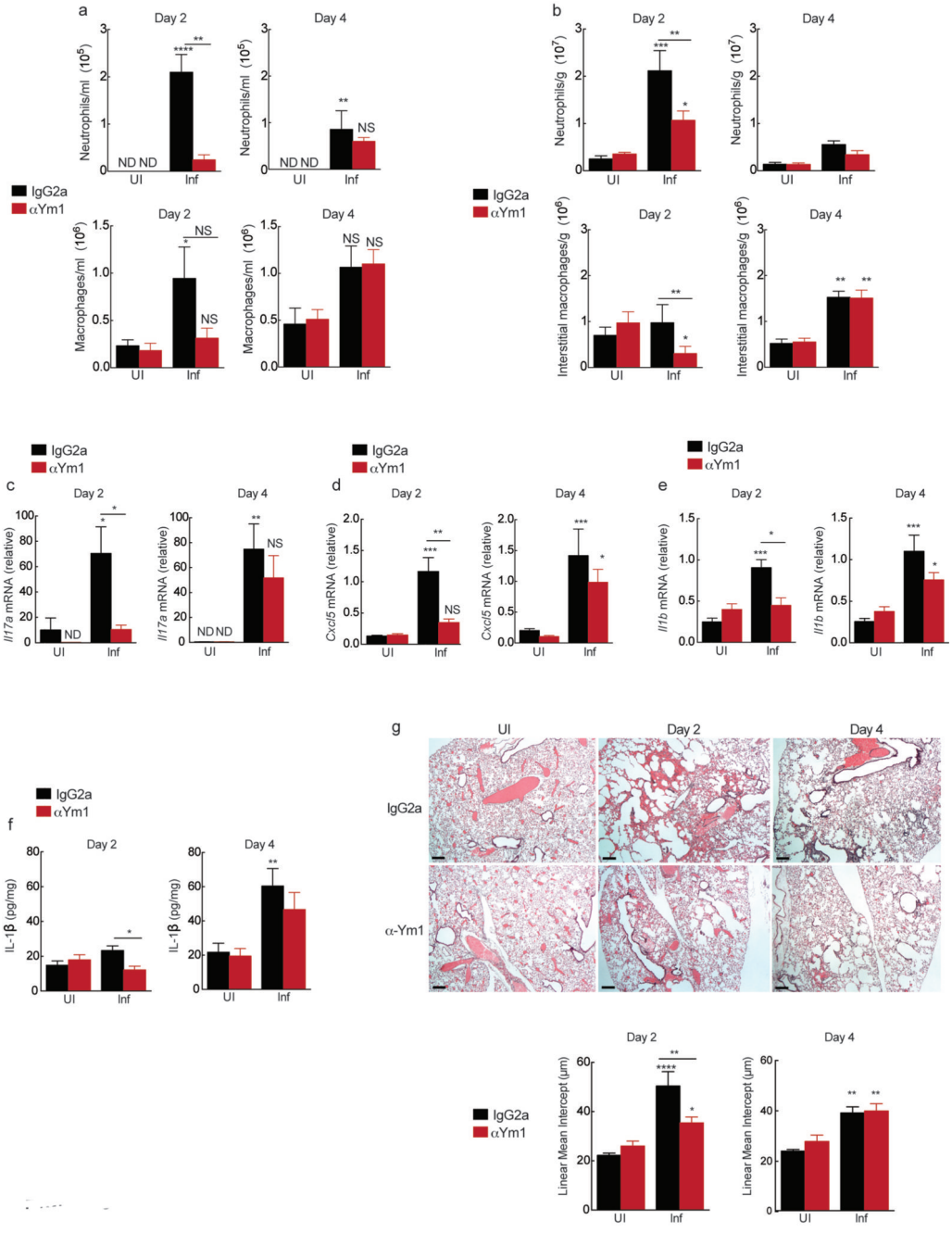

Figure 5. Ym1 induced neutrophil recruitment contributes to acute lung injury following *N. brasiliensis* infection

(**a**) Absolute numbers of neutrophil and macrophages in BAL counted on Diffquick stained cytospins from BALB/c mice uninfected (UI) or infected (Inf) with 500 *N. brasiliensis* L3s (day 0) and treated with anti-Ym1 or IgG2a isotype (i.p., days −1 to 1) harvested at day 2 or 4 after infection. (**b**) Absolute numbers of $Ly6G^+$ $Cd11b^+$ $F4/80^-$ neutrophils and $F4/80^+$ $Cd11b^+$ $CD11c^-$ interstitial macrophages per g of lung tissue from mice as in **a**. (**c-e**) Relative gene expression in lungs of mice as in **a**. (**f**) IL-1β per mg of total lung protein in lung homogenates from mice as in **a**. (**g**) H&E staining lung sections, scale bar: 200 μm.

Europe PMC Funders Author Manuscripts

Graph shows lung damage calculated by the linear means intercept. ND not detected. NS not significant; *$P < 0.05$; **$P < 0.01$; ***$P < 0.001$ and ****$P < 0.0001$ compared to UI IgG2a or Inf IgG2a (analysis of variance with Tukey-Kramer HSD multiple comparison test). All data are representative from three individual experiments (mean ± SEM, six mice per group).

Europe PMC Funders Author Manuscripts

Europe PMC Funders Author Manuscripts

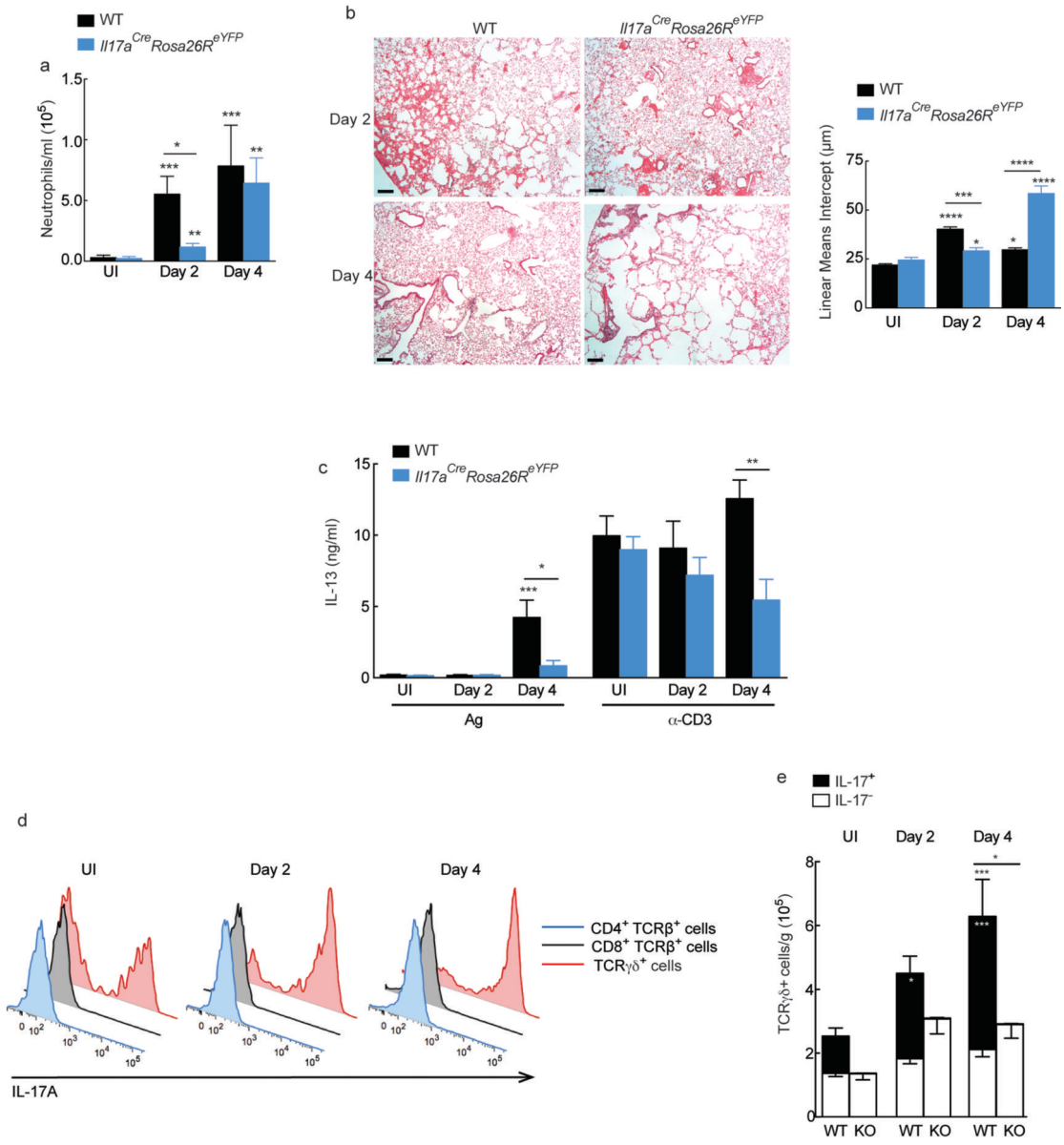

Figure 6. IL-17A production by γδ T cells contributes to *N. brasiliensis* mediated lung injury

(**a**) Absolute numbers of neutrophils in the BAL counted on DiffQuick stained cytospins from C57BL6 (WT) or homozygote *Il17a*^{Cre}*Rosa26R*^{eYFP} mice uninfected (UI) or infected with *N. brasiliensis* (500 L3s) harvested day 2 or 4 after infection. (**b**) H&E staining of lung sections from infected mice as in **a**; Scale bar: 200 μm. Graph shows lung damage calculated by the linear means intercept. (**c**) IL-13 secretion in splenocytes cultured with NES antigen (Ag; 1 μg/mL) or α-CD3 (1 μg/mL) from mice as in **a**. Data show Ag and α-CD3 specific responses normalized to the amount of IL-13 secreted in medium for individual mice. (**d**) Expression of IL-17A in PMA and ionomycin restimulated single cell lung suspensions from mice in **a**. (**e**) Absolute number of IL-17A^{-} or IL-17A^{+} TCRγδ^{+} cells uninfected or infected WT or *Il17a*^{Cre}*Rosa26R*^{eYFP} (KO) mice as in **a**. Statistics depicting significance of

IL-17A$^+$ γδ T cells in black, and total γδ T cells in white. NS not significant *P < 0.05; **P < 0.01; ***P < 0.001 and ****P < 0.0001 compared to UI WT or infected WT on day 2 or day 4 (analysis of variance with (**a**) Kruskal-Wallis or (**b-e**) Tukey-Kramer HSD multiple comparison test). Data are pooled (**a-c, e;** mean ± s.e.m.) or representative from two individual experiments of five to twelve mice per group.

Europe PMC Funders Author Manuscripts

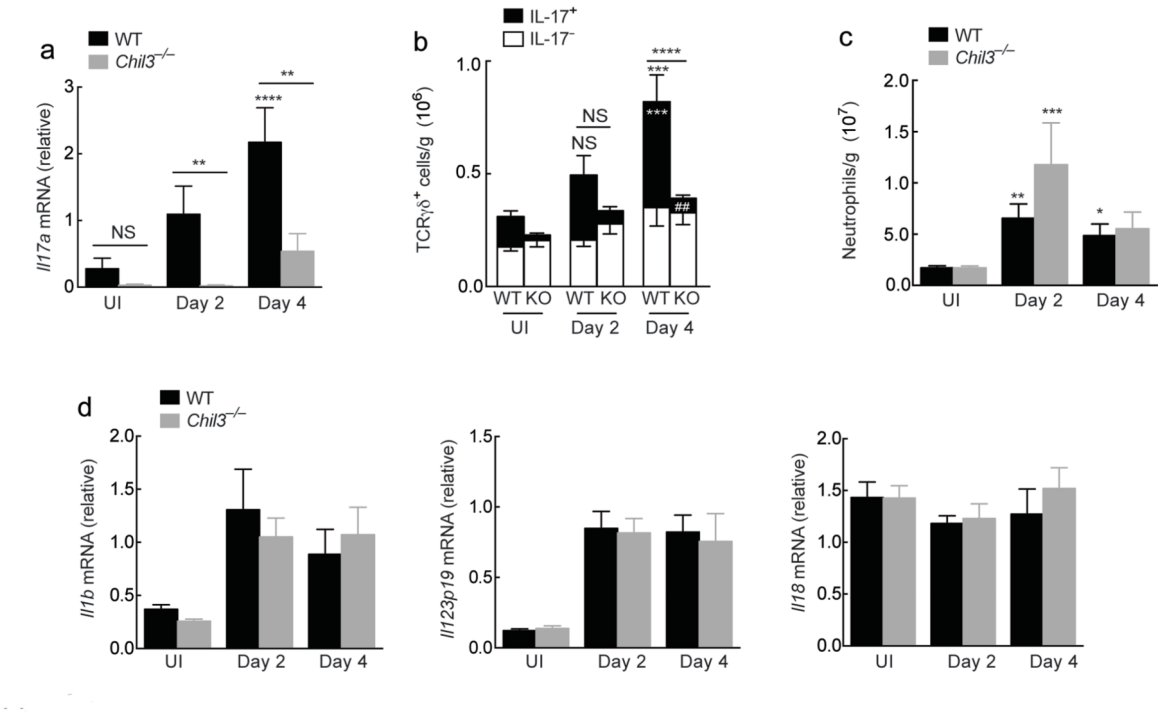

Figure 7. BRP-39 regulates IL-17A production in γδ T cells within the lung

(**a**) Relative gene expression in lungs of uninfected (UI) or *N. brasiliensis* infected (500 L3s) C57BL6 (WT) or *Chil1*$^{-/-}$ mice at day 2 or 4 after infection. (**b**) Absolute number of IL-17^{-} or IL-17^{+} γδ T cells following infection in WT or *Chil1*$^{-/-}$ (KO) mice as in **a**. Statistics depicting significance of IL-17A+ γδ T cells in black, and total γδ T cells in white. (**c**) Absolute numbers of Ly6G^{+} CD11b^{+} F4/80^{-} neutrophils per gram of lung tissue in WT and *Chil1*$^{-/-}$ mice as in **a**. (**d**) Relative gene expression in lungs of mice as in **a**. NS not significant; **P* < 0.05; ***P* < 0.01 and ****P* < 0.001, compared to UI WT or infected WT on day 2 or day 4 (**a-c**) and ##*P* < 0.01 compared to infected WT on day 4 (**c**) (analysis of variance with Tukey-Kramer HSD multiple comparison test). Data are representative of two individual experiments with twelve to six mice per group (mean ± s.e.m.).

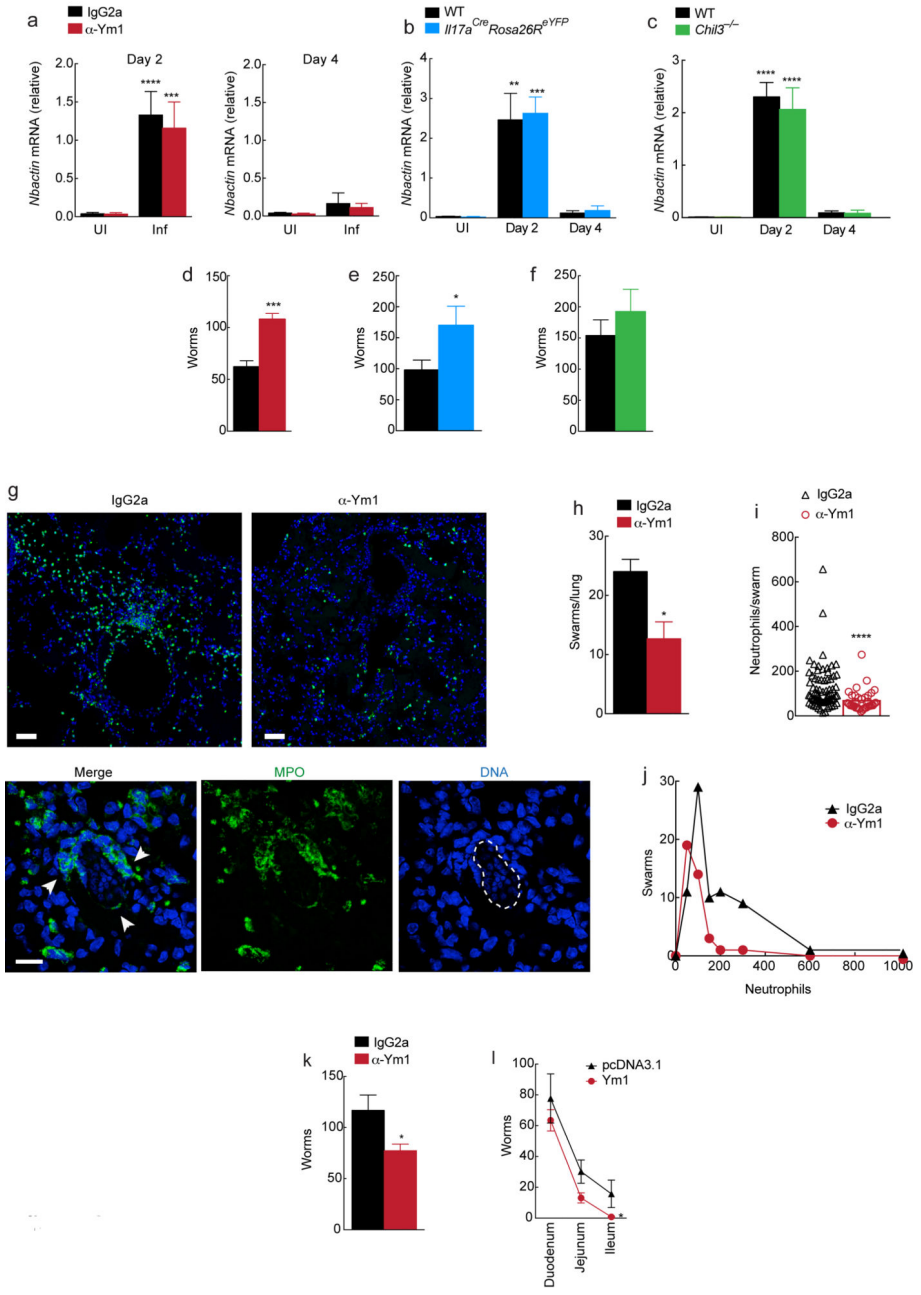

Figure 8. IL-17A and Ym1 limit worm burden

(**a-c**) Relative gene expression in whole lung tissue from uninfected (UI) or *N. brasiliensis* infected (Inf) (500 L3s) BALB/c wild-type treated with anti-Ym1 or IgG2a isotype (i.p., days -1 to 1) (**a**); C57BL6 (WT) or homozygote *Il17a*^{Cre}*Rosa26R*^{eYFP}(**b**); or C57BL6 (WT) or *Chil1*$^{-/-}$ mice (**c**) at day 2 or 4. (**d-f**) Larvae in the small intestine (day 4) in BALB/c mice (**d**) as in **a**; C57BL6 (WT) or homozygote *Il17a*^{Cre}*Rosa26R*^{eYFP} mice (**e**) as in **b**; C57BL6 (WT) or *Chil1*$^{-/-}$ mice (**f**) as in **c**. (**g**) Myeloperoxidase (MPO) and DAPI staining of lung sections from infected mice (day 2) as in **a**. White arrows, neutrophils; dotted line, *N. brasiliensis* larvae. Scale bar, 50 μm (top), 100 μm (bottom). (**h-j**) Lung sections from **g**

Europe PMC Funders Author Manuscripts

analyzed for (**h**) neutrophil swarms per section, (**i**) neutrophils per swarm; and (**j**) distribution frequency of neutrophils within swarms. (**k-l**) Larvae (day 4) in the (**k**) small intestine and (**l**) sections of the intestine of BALB/c wild-type mice transfected intranasally with pcDNA3.1 or plasmid encoding Ym1 and infected with *N. brasiliensis* (500 L3s). **P* < 0.05, ***P* < 0.01, ****P* < 0.001 and *****P* < 0.0001; (**a-c i**) analysis of variance with Tukey-Kramer HSD multiple comparison test; (**d-f**) unpaired *t*-test; (**h & i**) Wilcoxin non-parametric *t*-test. Data are representative of two independent experiments (**a-f;** six to eight mice per group, mean ± s.e.m.; **k-l**; nine mice per group, mean ± s.e.m.) or representative of one experiment with three mice per group (**g; h-j;** mean ± s.e.m.).

Europe PMC Funders Author Manuscripts

Table 1

Relative expression of CLP mRNA in the lung of mice

AAI Model	PBS challenge	OVA challenge
Chil1	0.88 ± 0.40	2.32 ± 0.50*
Chil3	1.06± 0.33	18.48 ± 2.83***
Chil4	0.20 ± 0.15	309.97 ± 11.53*

N. brasiliensis **model**	Uninfected	Day 2 after infection
Chil1	1.03 ± 0.12	1.85 ± 0.33
Chil3	1.03 ± 0.14	1.97 ± 0.27*
Chil4	5.93 ± 2.91	10634 ± 7227**

* *P* <0.05,

** *P* <0. 01 and

*** *P* <0.001 compared to PBS-challenge or uninfected mice (Students *t*-test). Data shows mean ± s.e.m. of individual mice from three independent experiments (PBS n=6; OVA n=9).